Mercury Species and SO_2 Adsorption on CaO(100)

Erdem Sasmaz and Jennifer Wilcox*

Department of Energy Resources Engineering, School of Earth Sciences, Stanford University, Green Earth Sciences 065, 367 Panama Street, Stanford, California 94305

Received: February 12, 2008; Revised Manuscript Received: July 26, 2008

First principles-based quantum mechanical tools based upon Density Functional Theory were used to investigate the binding mechanism of Hg species and SO_2 on CaO(100) surfaces for parallel and perpendicular orientations. One-fold, 2-fold and 3-fold high symmetry adsorption sites have been examined for the species, Hg^0, SO_2, HgCl, $HgCl_2$ and HgO. It has been discovered that HgCl, $HgCl_2$, and SO_2 are strongly adsorbed on the CaO(100) surface at 0.125 ML coverage with chemisorption as the likely adsorption mechanism. Binding energies of Hg^0 are minimal indicating a physisorption mechanism.

Introduction

Sulfur dioxide (SO_2) and mercury (Hg) are major atmospheric pollutants from coal combustion industries, and within the United States alone, 48 tons of mercury are released each year from coal burning.[1] In 2005, the Environmental Protection Agency (USEPA) adopted the Clean Air Mercury Rule to reduce mercury emissions from coal-fired power plants which will ultimately reduce U.S. emissions of mercury by 70%. Although this rule was vacated by congress in February 2008, roughly half of the states have existing mercury emissions controls in place for coal-fired power utilities.[2]

In flue gas desulphurization (FGD) processes, calcium-based sorbent materials are used to capture SO_2 from flue gas; however, calcium-based sorbents can also capture trace elements (TE) such as Hg, arsenic (As), and selenium (Se), in addition to SO_2.[3−15] Among all of these trace elements, elemental Hg causes the highest concerns, because it is more volatile and can easily pass through existing particulate control devices. Since FGD byproducts are used in gypsum production, which is then recycled to make wallboard and stucco materials, possible release of Hg might occur within the high-temperature recycling processes of gypsum.[16] Throughout the world, gypsum production is increasing steadily and the U.S. is the largest gypsum producer compensating 16.4% of world demand, with the world gypsum production being 102 million metric tons.[17−19] As the gypsum demand increases, it is essential to limit Hg capture in FGD processes to prevent the possible leaching of Hg in the recycling processes of FGD byproducts. Understanding the mechanisms associated with Hg and SO_2 adsorption will be crucial to limiting TE adsorption in FGD processes.

Mercury can exist in the elemental (Hg^0), oxidized (Hg^+, Hg^{2+}), or particulate (Hg_p) forms in the flue gas depending upon combustion conditions, the coal's chlorine content, and amount of hydrogen chloride (HCl). In addition, depending upon the temperature range of the quench zone, oxidized mercury can be found as mercuric chloride ($HgCl_2$) and mercuric oxide (HgO) at temperatures lower than 600 and 400 °C, respectively.[20,21] It is known that Hg^0 vapor is the dominant form compared to the oxidized form; however, Hg^0 reacts with acid species to form Hg^+ or Hg^{2+}.[22] Therefore, it is important to investigate the adsorption mechanism associated with the different forms of Hg to understand their behavior in the flue gas.

The content of commercially used Ca-based sorbents in FGD processes might vary with different compositions of CaO, calcium hydroxide ($Ca(OH)_2$), calcium carbonate ($CaCO_3$) and calcium sulfate ($CaSO_4 \cdot H_2O$).[8] In addition, Ca-based sorbents can be exposed to steam by which subsequent hydroxylation can lead to an increase in their reactivity. The reaction ($CaO + H_2O \leftrightarrow Ca(OH)_2$) between CaO and H_2O, being reversible and exothermic, occurs rapidly.[23] Kuborovic et al. found that the formation reaction of $Ca(OH)_2$ with water vapor equilibrates at approximately 740 K, and above this value the reaction proceeds in the direction of the reactant species, CaO and H_2O. The same reaction with water in the liquid phase yields a negative Gibbs free energy of reaction between 298 and 373 K, indicating that the reaction occurs in the direction of the product species, $Ca(OH)_2$.[24] Previous investigations indicate that water vapor enhances the reactivity[12,14] of Ca-based sorbents by increasing the rate of surface dissolution, thereby promoting stable complex formation at high vapor pressures.[14,15] In this study, the interaction of flue gas species with clean a CaO(100) surface has been examined and mechanisms associated with the adsorption of SO_2 and Hg species including Hg^0, Hg^+ (HgCl), Hg^{2+} ($HgCl_2$ and HgO) on CaO(100) are reported. Since previous investigations have clearly indicated the importance of adsorption based upon the influence of water, the inclusion of water will be considered in future studies. The current study provides insight to the fundamental chemical reactivity and corresponding mechanisms of calcium oxide, sulfur, and mercury interactions based upon first-principle density functional theory (DFT) calculations. There have been additional theoretical investigations regarding the structure of calcium oxide using both cluster and periodic approaches in the literature.[25−30] However, none of these studies have examined the adsorption of Hg and its species, specifically.

Computational Methodology. The DFT-based geometry optimization and total energy calculations were obtained using the plane-wave-based Vienna ab initio Simulation Package[31−33] (VASP). It has been suggested that for heavy elements such as Hg, DFT calculations can be computationally demanding since both relativistic and correlation effects need to be included for accurate geometry and energy predictions.[34−36] Ultrasoft Vanderbilt pseudopotentials were used to describe the core orbitals[37,38]

* To whom correspondence should be addressed. Tel: 650-724-9449. Fax: 650-725-2099. E-mail: wilcoxj@stanford.edu.

10.1021/jp801250h CCC: $40.75
Published on Web 09/25/2008

TABLE 1: Spectroscopic Parameters for the Hg_2 Dimer, HgCl, and $HgCl_2$

	Hg_2		HgCl		$HgCl_2$	
	DFT	exptl	DFT	exptl	DFT	exptl
bond length (Å)	3.61	3.69[a]	2.45	2.36−2.50[b,c,d,e]	2.286	2.25−2.44[b,c,d,e,g,h,j,f]
dissoc. energy (eV)	−0.05	−0.047[a]	−1.18	−1.01[f]	−4.702	−4.68[k]
frequencies (cm^{-1})	21.8	19.7[a]	263.71	292.61[g]	343, 393	353, 402.5[l]

[a] Reference 41. [b] References 42−45. [c] References 42−45. [d] References 42−45. [e] References 42−45. [f] Reference 46. [g] Reference 47. [h] References 48−50. [j] References 48−50. [k] Reference 51. [l] Reference 52.

and electron exchange correlation functionals were calculated using the Perdew and Wang[39] approximation which was described using the generalized-gradient approximation (GGA). To test the accuracy of the pseudopotentials, bond length (r), dissociation energy (D_e) and harmonic vibrational frequency (ω_e) of the Hg_2 dimer, HgCl and $HgCl_2$ have been calculated and compared against experimental data, as illustrated in Table 1. For these test calculations, a plane-wave expansion with a cutoff energy of 350 eV was employed for Hg and Cl. The residual minimization method for relaxation was performed with a single k-point. From Table 1 it is clear that the vibrational frequency calculated for the Hg_2 dimer, HgCl and $HgCl_2$ are in reasonable agreement with experiment with a deviation of approximately 2, 30 and 10 wavenumbers, respectively. Predicted bond lengths and dissociation energies agree well with the experimental data, with the exception of the dissociation energy of HgCl, which deviates 0.17 eV from experiment.

DFT can yield reliable predictions for the structure of CaO provided the cutoff energies and density of k-points within the Brillouin zone are determined accurately through a convergence check of the total energy of the slab calculations.[28] However, CaO has a wide band gap (7.1 eV)[53] and it is well-known that both the local density approximation (LDA) and generalized-gradient approximation (GGA) underestimate the band gap of CaO[54−57] due to the neglect of the strong polarization of the charge density of the molecule and the strong on-site Coulomb repulsion between the d electrons.[58,59] Calcium oxide is a nonmagnetic insulating oxide that has a strongly correlated electronic structure. Using a hybrid functional[60] or by adding a Hubbard term that defines the strong on-site Coulomb (U) and exchange interaction (J) parameters[61] to the GGA Hamiltonian, can improve band gap and magnetic moment predictions of metal oxides.[60−62] Additionally, the GW approximation was used to calculate the self-energy to account for the Coulomb and exchange interactions for CaO and predicted a bandgap of 6.64 eV.[63] Within the current investigation, the band gap of bulk CaO has been calculated as 3.54 eV with GGA, which is consistent with other DFT-based studies.[54,57,58] It has been reported that GGA provides reasonably accurate lattice constants and cohesive energies, but underestimates band gaps and magnetic moments.[61] GGA gives similar or slightly higher binding energies in comparison to GGA+U approach on metal oxide surfaces, because of its inability to define Coulomb repulsion.[61,64−66] The current investigation is the first of its kind to examine the adsorption phenomena of coal combustion flue gas species on CaO using DFT. Future studies will involve these higher-order methods, but trends and mechanisms of adsorption can be determined by the present study.

The CaO(100) surface has been modeled using periodic slabs of CaO with three-dimensional boundary conditions. Each slab is separated from one another by at least a 10 Å-thick vacuum layer to minimize interactions between the slabs. For all surfaces, a cutoff energy of 520 eV has been used to calculate binding energies. In addition, for the relaxation of the structure, a Gaussian-smearing width of 0.1 eV was used to gain further accuracy. Geometry relaxation calculations employed the conjugate-gradient (CG) algorithm until the forces on the unconstrained atoms were less than 0.03 eV/Å. To validate the accuracy of the calculations, binding energies of Hg^0 and HgCl have been calculated as a function of slab layers and k-point mesh size created by a Monkhorst−Pack mesh.[40] Further details are provided in the Supporting Information. Although the larger $5 \times 5 \times 1$ and $7 \times 7 \times 1$ k-point mesh sizes have been employed for HgCl and Hg^0 with two-, three-, four- and five-slab layers, it has been found that two slab layers with smaller k-point mesh sizes yields reasonable accuracy with binding energies of Hg^0 and HgCl changing by less than 0.0035 and 0.0566 eV, respectively. In addition, the CaO surface has been modeled with two different surface structure configurations, i.e., 2×2 surface cells with a grid size of $3 \times 3 \times 1$ k-points and $2\sqrt{2} \times 2\sqrt{2}$ surface cells with a grid size of $2 \times 2 \times 1$ k-points. Due to the high number of atoms in the $2\sqrt{2} \times 2\sqrt{2}$ surface cell, a smaller k-point mesh size has been applied. Adsorption studies on smaller surface cells such as 1×1 and $\sqrt{2}x\sqrt{2}$ have also been carried out; however, it has been discovered that the smaller surface cells are not large enough for parallel-lying binding with larger molecules such as SO_2, HgCl, $HgCl_2$, and HgO. Comparing the bond lengths of the surface atoms, i.e., Ca−O (2.4 Å), with the adsorbate molecules O−S−O (1.47 Å), Hg−Cl (2.36−2.50 Å), Cl−Hg−Cl (2.25−2.44 Å), and Hg−O (2.04 Å), one can conclude that adsorption with large surface coverage ratios may not be possible, unless the adsorbates dissociate on the CaO surface. For all of the calculations, single molecules have been placed on the surface corresponding to a coverage of $\Theta = 0.25$ ML for the 2×2 surface cells and $\Theta = 0.125$ ML for the $2\sqrt{2} \times 2\sqrt{2}$ surface cells. The binding energies (E_{bind}) of the flue gas components on the CaO surfaces were calculated according to eq 1

$$E_{bind} = E_{AB} - [E_A + E_B] \quad (1)$$

where AB, A, and B represent adsorbate/substrate, adsorbate, and substrate systems, respectively.

Results and Discussion

Energies of the CaO structure were calculated using different lattice constants according to the CaO space group. Ground state energies were then obtained from plots of the energy versus lattice constant, by choosing the minimum energy. The lattice constant of the CaO structure was found to be 4.773 Å, which agrees well with experiments of Mehl et al. (4.81 Å).[67]

Hg^0 Binding on CaO(100). The binding mechanism of Hg^0 has been investigated using both the small (2×2) and large ($2\sqrt{2} \times 2\sqrt{2}$) surface cells of CaO. Elemental mercury is initially placed on different adsorption sites, i.e., bridge, hollow, top-O_s, and top-Ca, on the CaO surface, as shown in Figure 1. Binding energies and bond lengths between the surface atoms and Hg^0 on these adsorption sites have been calculated and are

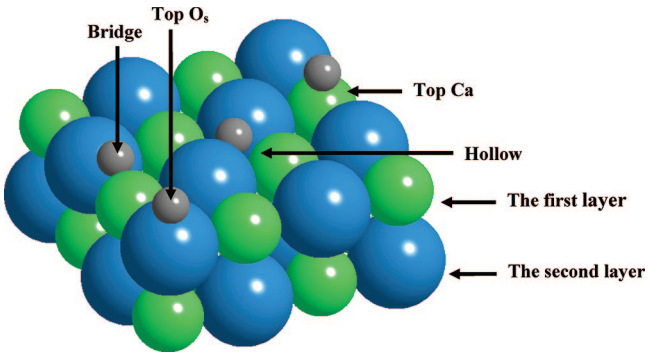

Figure 1. Illustration of high-symmetry adsorption sites of CaO(100), including the bridge site, hollow site, top O_s site and top Ca site.

TABLE 2: Binding Energies (eV) and Bond Lengths (Å) between Surface Atoms and Hg^0 on Different Adsorption Sites of CaO(100)

	2 × 2 surface cell			$2\sqrt{2} \times 2\sqrt{2}$ surface cell		
	E_{bind}	r(Ca−Hg)	r(O_s−Hg)	E_{bind}	r(Ca−Hg)	r(O_s−Hg)
bridge	−0.114	3.384	3.160	−0.122	3.561	3.160
hollow	−0.117	3.608	3.599	−0.121	3.570	3.527
top Ca	−0.095	3.484	4.224	−0.087	3.542	3.785
top O_s	−0.122	3.871	3.036	−0.127	3.861	3.045

presented in Table 2. The binding energies change minimally between 0.087 and 0.127 eV and as the surface coverage is decreased, the binding energy of Hg^0 increases slightly due to a decreased interaction of neighboring Hg atoms on the surface. However, the effect of surface coverage change is not seen on the top-Ca sites which may be due to the instability of the top-Ca sites. Higher binding energies were calculated when the bond length between surface Ca and Hg^0 atoms was longer and the bond length between surface O (O_s) and Hg^0 atoms was shorter. In addition, as demonstrated in Figure 2 and Table 2, optimized geometries of Hg^0 binding on CaO(100) for both 2 × 2 and $2\sqrt{2} \times 2\sqrt{2}$ surface cells indicate that Hg^0 has a preferred interaction with the surface oxygen atom. The highest binding energy of Hg^0 calculated was 0.127 eV, which constitutes a weak interaction. The likely binding mechanism of Hg^0 to CaO is physisorption. This result is consistent with experiments reporting that elemental mercury may not be adsorbed by calcium-based sorbents[8,9] until it is first oxidized. The oxidized forms of Hg, i.e., HgCl, $HgCl_2$, and HgO were also investigated in the following sections, in addition to SO_2 binding.

SO_2 Binding on CaO(100). The binding mechanism of SO_2 on CaO(100) has been investigated using both 2 × 2 and $2\sqrt{2} \times 2\sqrt{2}$ surface cells. Sulfur is initially placed parallel and perpendicular to the surface atoms on bridge, 4-fold hollow, top-O_s and top-Ca adsorption sites. Although the adsorbate is located on different adsorption sites initially, just one stable geometry is obtained on the surface for each parallel and perpendicular orientation. Calculated binding energies and bond lengths of SO_2 on the most stable location are illustrated in Table 3 and within the Supporting Information. It has been determined that SO_2 prefers a parallel orientation to the surface with a high binding energy showing a likely chemisorption mechanism. As demonstrated in Figure 3, when SO_2 is parallel to the surface, sulfur interacts with the O_s atom while the oxygen atoms of SO_2 stay closer to the Ca atoms. It can be concluded that sulfur does not prefer to be located at top-sites of Ca atoms and the position of SO_2 changes when sulfur is initially located at top-Ca sites. Additionally, when SO_2 adsorbs parallel to the surface, the top O_s sites are preferred, exhibited by a decrease in the bond angle formed between S and O, e.g., from 120° to 111°. For perpendicular orientations, SO_2 binds to the CaO surface as shown in Figure 4. However, this interaction is very weak compared to the parallel orientation and adsorption via this pathway is likely not preferred. As the surface coverage decreases to 0.125 ML of SO_2, the binding energy of SO_2 increases by approximately 0.3 eV in the parallel orientation and changes only slightly in the perpendicular orientation. The reason for the increase of the parallel orientation is due to a decreased repulsive interaction between adsorbate molecules. The adsorbed atoms will affect the orbitals of neighboring surface atoms making them less reactive for a second atom. Examination of these strong binding energies indicates chemisorption behavior, which suggests that a reaction might occur between SO_2 and CaO. The current results agree with the theoretical results of Pacchioni et al.[30] who studied the adsorption of SO_2 on CaO(100) surfaces using $[OCa_5]^{8+}$ clusters embedded within an array of point charges. They reported that the orientation of adsorbed SO_2 was parallel to the surface where the sulfur atom remains perpendicular to the O^{2-} anion and conclude that SO_2 formed stable surface sulfites on CaO(100) with a dissociation energy of more than 1 eV.

HgCl Binding on CaO(100). Binding energies of HgCl on CaO(100) were calculated in a similar manner to those of SO_2 and Hg^0, with the bond distances of the most stable geometries listed in Table 3 and within the Supporting Information. It has been observed that binding energies of HgCl on unique adsorption sites are similar to one another. The molecule HgCl moves to different stable positions leaving the initially located adsorption sites for both parallel and perpendicular orientations on CaO(100). As demonstrated in Figure 3, the parallel orientation of the Hg atom is at the top O_s site while the Cl atom stays closer to Ca with a bond distance of 2.60 Å with Hg. This bond distance is slightly higher than its experimental gas-phase value (2.36−2.50 Å), showing the possible bond stretch of HgCl on the CaO surface. In Figure 4, the optimized geometry for the perpendicular orientation of HgCl is illustrated. It has been found that Hg is bound to the Cl atom with a weak interaction and not bound to the surface, while Cl on the other hand, interacts with both Ca and O_s and remains closer to the surface. It has been observed that the bond length between Cl and O_s is closer than the Cl−Ca bond length, which indicates a preferred Cl−O interaction over that of Cl−Ca. Another possible configuration for the perpendicular adsorption of HgCl on the CaO(100) surface is with the Hg atom located closer to the surface. However, this scenario results in a weak interaction with a binding energy of approximately −0.1 eV for all possible adsorption sites. Calculated binding energies on different surface cells showed that a perpendicular orientation of HgCl is favorable compared to the parallel adsorption of HgCl at high surface coverage; however, the exact opposite trend is observed at low surface coverage. Again, it is hypothesized that this is due to a decreased interaction between HgCl molecules on the CaO surface. A potential energy diagram of HgCl adsorption and potential desorption on CaO(100) at coverages of 0.25 ML has been calculated, as shown in Figure 5. Free energies of adsorbed molecules HgCl, Hg^0 and Cl have been normalized to the sum of free energies of the CaO(100) surface and HgCl(g). The stable states are connected with dotted lines, but the transition states connecting these stable species have not been calculated. Figure 5 illustrates that in both parallel and perpendicular orientations, the adsorption of HgCl is more likely to happen in comparison to two possible HgCl dissociation scenarios, i.e., Hg adsorbs on the surface and Cl desorbs or Cl

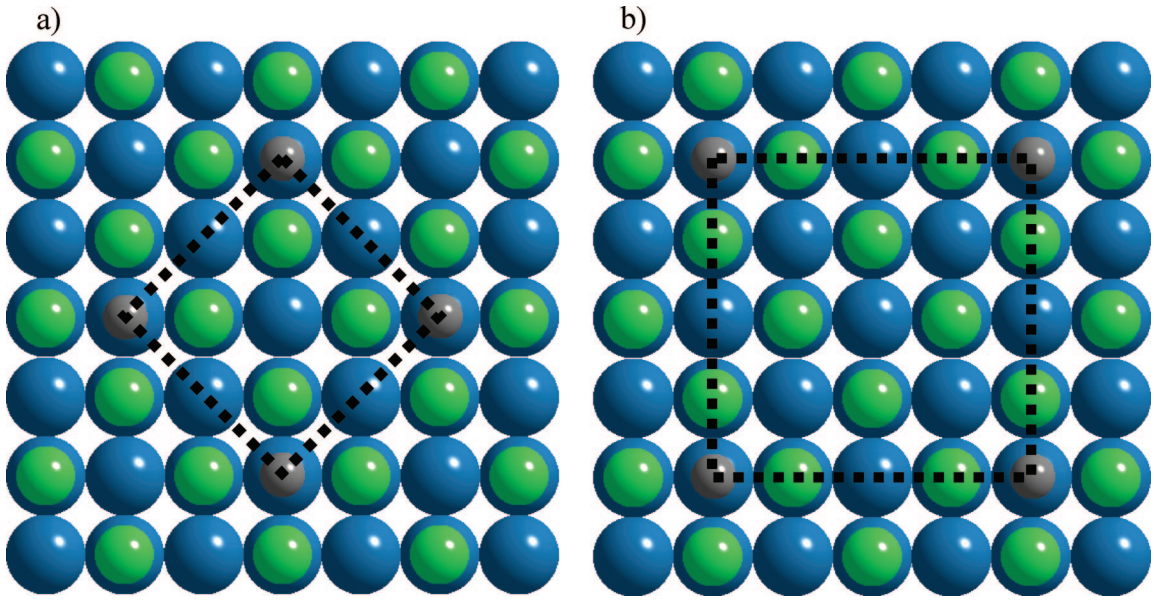

Figure 2. Models for Hg adsorption on top O_s of CaO(100) surface (a) CaO(100) (2 × 2)-Hg-0.25 (b) CaO(100) (2√2 × 2√2)R45°-Hg-0.125 (Atoms are represented as Ca, green; O, blue; Hg, gray).

TABLE 3: Binding Energies and Adsorption Sites of SO_2, HgCl, $HgCl_2$, and HgO Molecules for Parallel and Perpendicular Orientations on 2 × 2 and 2√2 × 2√2 Surface Cell of CaO(100)

	2 × 2 surface cell		2√2 × 2√2 surface cell	
	parallel	perpendicular	parallel	perpendicular
SO_2	−1.474	−0.288	−1.75	−0.28
−S	top O_s	−	top O_s	−
−O	bridge	bridge	bridge	bridge
HgCl	−0.879	−0.905	−1.04	−0.924
−Hg	top O_s	−	top O_s	−
−Cl	top Ca	top O_s	top Ca	top O_s
$HgCl_2$	−0.793	−0.326	−0.932	−0.33
−Hg	top O_s	−	top O_s	−
−Cl	top Ca	top O_s	top Ca	top O_s
HgO	−1.38	−2.757	−1.531	−2.763
−Hg	top O_s	−	top O_s	−
−O	top Ca	top O_s	top Ca	top O_s

adsorbs on surface and Hg desorbs. Since the first scenario is highly endothermic (1.09 eV), it will not occur during the adsorption of HgCl; however, the second scenario is exothermic (−0.75 eV) with a likelihood of occurring. In comparison to the adsorption of HgCl for both parallel and perpendicular orientations, the adsorption of Cl and desorption of Hg is 0.13 and 0.16 eV more endothermic than these orientations, respectively. This small energy difference indicates that the surface interaction with Cl causes a decrease in the interaction between Cl and Hg leading to the stretch of the HgCl bond and possible desorption of Hg, where as Cl is strongly bound to O_s sites on the surface. It can be concluded that the high binding energy of HgCl is representative of chemisorption behavior between HgCl and the CaO(100) surface at 0.25 ML coverage; however, these energies might also represent desorption of Hg and the interaction of Cl atoms with CaO(100). A low surface coverage ratio is necessary for HgCl adsorption to take place on CaO surfaces.

$HgCl_2$ Binding on CaO(100). The binding energies and bond distances of the most stable geometries of $HgCl_2$ calculated on 2 × 2 and 2√2 × 2√2 surface cells are shown in Table 3 and in the Supporting Information. For the parallel cases, optimized geometries of $HgCl_2$ remain almost parallel to the surface. The molecule $HgCl_2$ is linear; however, the angle between Hg and Cl decreases to 160° and the bond length between Hg and Cl increases with surface interactions. As seen in Figure 3, Hg migrates to the top-O_s site, while the two Cl atoms are stable at the top-Ca sites. This observation indicates that both sites play a role in the adsorption of $HgCl_2$. An experimental study conducted by Gullet et al.[8] is in agreement with this conclusion, and reports that $HgCl_2$ can be captured in parallel on CaO with the attraction of both the acidic (Ca^{2+}) and basic (O^{2-}) sites. On the other hand for perpendicular cases, as shown in Figure 4, $HgCl_2$ maintains its linearity and experimental bond length on the surface. The molecule $HgCl_2$ is bound with the Cl atom interacting with the top-O_s site, having a bond angle of 80° with the surface. The comparison of binding energies of both parallel and perpendicular cases demonstrates that perpendicular adsorption of $HgCl_2$ is not stable on the CaO(100) surface. Decreasing the surface coverage causes a 0.14 eV increase in the binding energy of $HgCl_2$ in the parallel orientation, and only a slight change in the perpendicular orientation. It has been determined that a decreased interaction between $HgCl_2$ molecules at low surface coverage has no effect on the binding energy of $HgCl_2$ in the perpendicular orientation. Also, it is important to recognize that SO_2 and $HgCl_2$ both have a preference to bind at the top-O_s sites. Therefore, it is possible for these species to compete for adsorption sites, and a comparison of the binding energies of $HgCl_2$ and SO_2 indicate that the parallel sulfur binding is stronger.

HgO Binding on CaO(100). The binding energies and bond distances of the most stable geometries of HgO calculated on 2 × 2 and 2√2 × 2√2 surface cells are shown in Table 3 and in the Supporting Information. The binding mechanisms of HgO and HgCl on CaO(100) show similar behavior. The bond length of HgO increases as HgO approaches the CaO surface in the perpendicular orientation, which is shown in Figure 4. The Hg atom stays away from the surface with a bond distance of approximately 4 Å. This behavior is not observed for the parallel orientation case. Since the 4-fold hollow and top-O_s sites are favorable adsorption sites for Hg^0, it has been thought that O and Hg might compete for these sites. If O approaches the top-O_s it repulses Hg; however, if Hg approaches the top-O_s sites, Hg and O maintain their interaction. In addition, they are bound

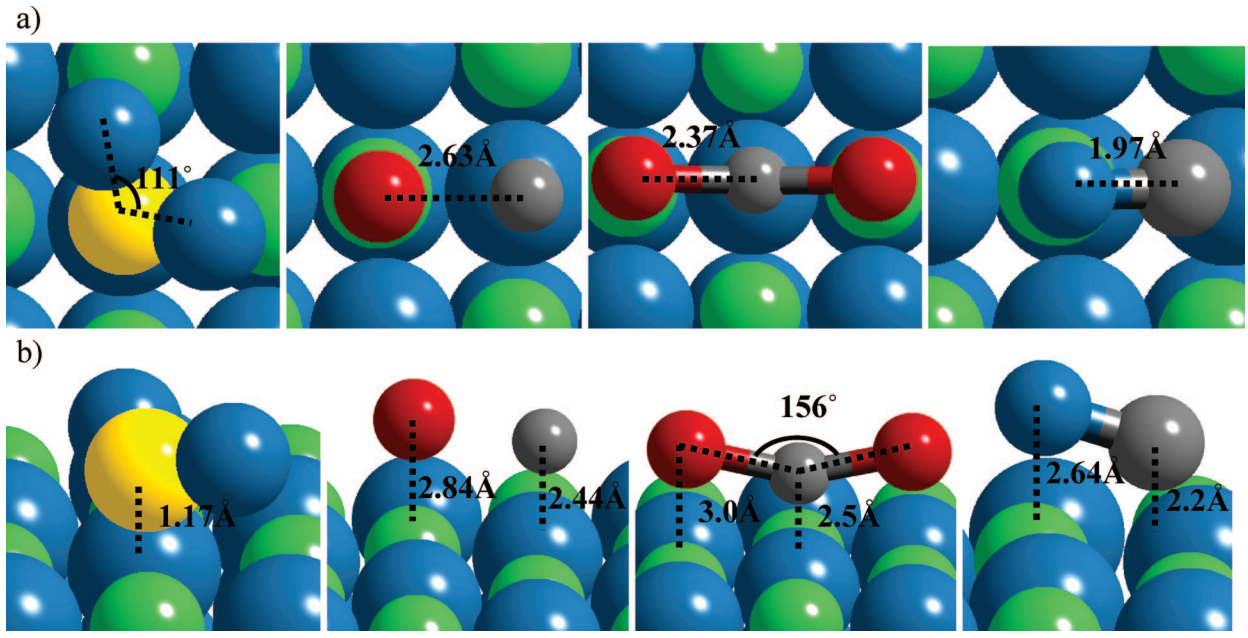

Figure 3. Most stable optimized geometries of SO_2, HgCl, $HgCl_2$, and HgO on CaO(100) surface, where molecules are parallel to the surface (a) top view (b) side view. (Atoms are represented as Ca, green; O, blue; S, yellow; Hg, gray; Cl, red).

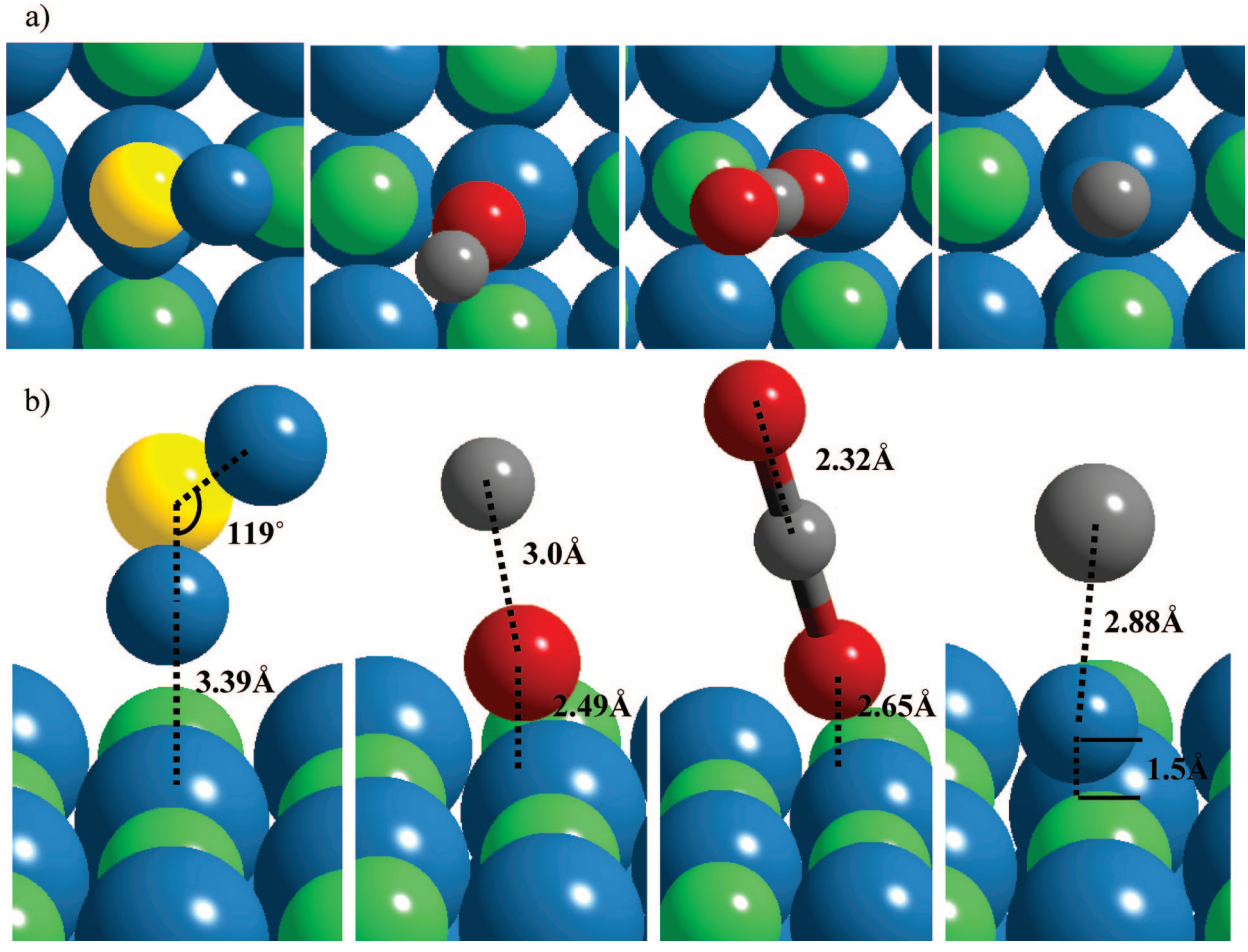

Figure 4. Most stable optimized geometries of SO_2, HgCl, $HgCl_2$, and HgO on CaO(100) surface, where molecules are perpendicular to the surface (a) top view (b) side view. (Atoms are represented as Ca, green; O, blue; S, yellow; Hg, gray; Cl, red).

to Ca and O_s atoms, respectively and the bond length of HgO is not affected by the surface interactions. All of these observations represent the nondissociative adsorption of HgO on CaO(100). However, the binding energies in Table 3, indicate that the $O-O_s$ interaction in the perpendicular orientation is approximately two times higher than the $Hg-O_s$ interaction in the parallel orientation; therefore, the dissociation of HgO with the binding of O on the CaO(100) surface is likely the dominant interaction pathway, rather than the combined interaction of HgO on the surface. Another possibility of perpendicular adsorption

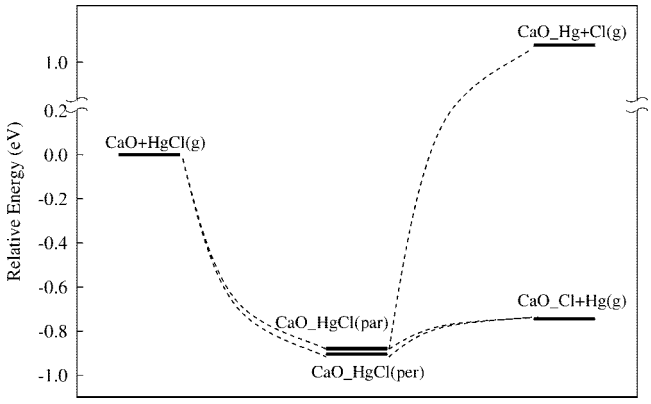

Figure 5. Potential energy diagram for different pathways of HgCl on CaO(100). Energies are relative to the sum of the energies of bare CaO and HgCl(g).

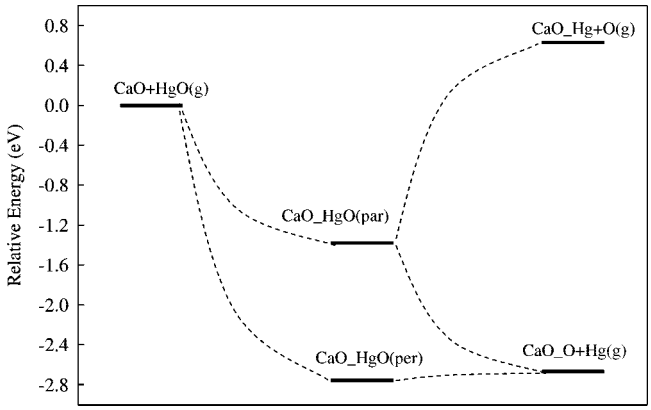

Figure 6. Potential energy diagram for different pathways of HgO on CaO(100). Energies are relative to the sum of the energies of bare CaO and HgO(g).

of HgO on CaO(100), where Hg atoms are closer to the surface has also been carried out, but a very weak interaction has been observed with the surface and Hg. Decreasing the surface coverage ratio results in a 0.2 and 0.006 eV increase in the binding energies of HgO in the parallel and perpendicular orientations, respectively. It has been noted that although more active sites exist for the adsorption of HgO at low surface coverage, the dissociation of HgO is still more favorable than the combined interaction of HgO with the surface. Additional calculations have been carried out to investigate the dissociation of HgO and desorption of Hg from the surface at 0.25 ML coverage. Figure 6 illustrates the potential energy diagram of HgO on the CaO(100) surface prepared with the same methodology explained in above section. The energy of HgO adsorbed in the perpendicular orientation is only 0.09 eV lower than that of the single O atom adsorbed with Hg desorbed from CaO surface. This small difference shows that the simultaneous binding of Hg and O atoms to the surface may not be stable. Additionally, the adsorption of Hg and desorption of O from the CaO surface are highly endothermic and is likely not to occur on the CaO(100) surface.

Conclusions

The binding mechanisms of SO_2 and Hg species have been investigated on CaO(100) surfaces with both parallel and perpendicular orientations to the surface considered. Binding energies of these species are calculated for different adsorption sites and the most favorable adsorption sites have been found. It can be concluded that SO_2 is strongly adsorbed by the CaO(100) surface and that chemisorption is likely the adsorption mechanism. The oxidized form of mercury, HgCl is adsorbed on the CaO(100) surface at low coverage; however, free energy calculations indicate that HgO may not be stable on the surface, resulting in the desorption of elemental mercury. The other oxidized form of mercury, $HgCl_2$, forms a more stable complex on the surface and interacts with the acidic and basic sites of CaO(100). Although its binding is not as strong as that of HgCl, a comparison of binding energies indicates that this compound might remain on the surface with the two adsorption sites reinforcing its stability. Elemental mercury binds weakly to the CaO(100) surface indicating a physisorption mechanism. It is important to note that some of the binding energies predicted in this work may be upper estimates due to the inability of the GGA to account for the on-site Coulomb repulsion between the d electrons.

Acknowledgment. The authors thank Dr. Shela Aboud for her valuable discussions and suggestions. The computations were carried out on the Stanford CEES (Center for Computational Earth and Environmental Science) grid.

Supporting Information Available: Additional bond length and bond energy data. This material is available free of charge via the Internet at http://pubs.acs.org.

References and Notes

(1) Mercury Study Report to Congress, US Environmental Protection Agency: Research Triangle Park, NC, 2003.

(2) The Clean Air Mercury Rule. www.epa.gov/air/mercuryrule (accessed May 2008)

(3) Sakai, M.; Su, C.; Sasaoka, E. *Ind. Eng. Chem. Res.* **2002**, *41*, 5029–5033.

(4) Jozewicz, W.; Chang, J. C. S.; Brna, T.; Sedman, C. *Environ. Sci. Technol.* **1987**, *21*, 664.

(5) Lee, K. T.; Bhatia, S. *J. Mater. Cycles Waste Manag.* **2005**, *7*, 16–23.

(6) Ho, T. C. *Control of Trace Metal Emissions during Coal Combustion, Final Technical Report*, 1998, Lamar University, Texas.

(7) Hartman, M.; Trnka, O. *AIChE J.* **1993**, *39* (4), 615–24.

(8) Gullet, B. K.; Ghorishi, B.; Keeney, R.; Huggins, F. E. *Mercuric Chloride Capture by Alkaline Sorbents, Proc. Air & Waste Management Association 93 rd. Annual Meeting* 2000, Salt Lake City, UT.

(9) Niksa, S.; Fujiwara, N. *The Impact of Wet FGD Scrubbing on Hg Emissions From Coal-Fired Power Stations. Proc. U.S. EPA-DoE-EPRI Combined Power Plant Air Pollutant Control Symp: The MEGA Symp* 2004, Washington, DC.

(10) Diaz-Somoano, M.; Martinez-Tarazona, M. R. *Environ. Sci. Technol.* **2004**, *38*, 899–903.

(11) Krishnan, S.V.; Bakhteyar, H.; Sedman, C. B.; *89th Air Waste Management Association Annual Meeting,* 1996, Nashville, Tennessee.

(12) Lancia, A.; Musmarra, D.; Pepe, F.; Volpicelli, G. *Combust. Sci. Technol.* **1993**, *93*, 277.

(13) Ghosh-Dastidar, A.; Mahuli, S.; Agnihotri, R.; Fan, L.-S. *Environ. Sci. Technol.* **1996**, *30*, 447–452.

(14) Bausach, M.; Pera-Titus, M.; Fite', C.; Cunill, F.; Izquierdo, J.-F.; Tejero, J.; Iborra, M. *AIChE J.* **2005**, *51* (5), 1455–66.

(15) Bausach, M.; Pera-Titus, M. ; Tejero, J.; Cunill, F. *Chem. Lett.* **2006**, *35* (1),

(16) 2004 Coal Combustion Product Survey. American Coal Ash Association. http://www.ACAA-USA.org

(17) Founie, A. U.S. *Geological Survey Minerals Yearbook, Gypsum* **2003**,

(18) Engineering News-Record, 2003 Construction economics: 250 (24), 24−26.

(19) Engineering News-Record, 2003 Construction economics: 250 (3), 24−26.

(20) Diaz-Somoano, M.; Unterberger, S.; Hein, K. R. G. *Fuel* **2006**, *85*, 1087–1093.

(21) Licata, A.; Balles, E.; Schuttenhelm, W. *Mercury Control Alternatives for Coal-Fired Power Plants, Power Gen* **2002**, Orlando, December 2002.

(22) Hutson, N.; Singer, C.; Richardson, C.; Karwowski, J.; Sedman, C. *Practical Applications from Observations of Mercury Oxidation and*

Binding Mechanism. Proc. U.S. *EPA-DOE-EPRI Combined Power Plant Air Pollutant Control Symp: The MEGA Symp* **2004**, Washington, DC.
(23) Song, C. H. *Kim. Cement Concrete Res.* **1990**, *20*, 815.
(24) Kuburovic, M.; Duric, S.; Jovovic, A.; Karan, M. *Thermal Sci.* **2002**, *6*, 71.
(25) Wang, C.; Zhang, S.; Chen, N.-X. *J. Alloys Compd.* **2005**, *338*, 195.
(26) Malliavin, M.-J.; Coudray, C. *J. Chem. Phys.* **1997**, *106*, 6.
(27) Konigstein, M.; Catlow, C. R. *J. Solid State Chem.* **1998**, *140*, 103.
(28) De Leeuw, N. H.; Purton, J. A. *Phys. Rev. B* **2001**, *63*, 195417.
(29) Bawa, F.; Panas, I. *Chem. Phys.* **2001**, *3*, 3042.
(30) Pacchioni, G.; Ricart, J. M.; Illas, F. *J. Am. Chem. Sci.* **1994**, *116*, 10152–10158.
(31) Kresse, G.; Hafner, J. *Phys. Rev. B* **1993**, *48*, 13–115.
(32) Kresse, G.; Hafner, J. *Phys. Rev. B* **1994**, *49*, 14251.
(33) Kresse, G.; Furthmuller, J. *Comput. Mater. Sci.* **1996**, *6*, 15.
(34) Schwerdtfeger, P.; Wesendrup, R.; Moyano, G. E.; Sadlej, A. J.; Greif, J.; Hensel, F. *J. Chem. Phys.* **2001**, *115* (16), 7401–11.
(35) Kresse, G.; Hafner, J. *Phys. Rev. B* **1997**, *55* (12), 7539–48.
(36) Gaston, N.; Schwerdtfeger, P. *Phys. Rev. B* **2006**, *74*, 024105.
(37) Vanderbilt, D. *Phys. Rev. B* **1990**, *41*, 7892.
(38) Kresse, G.; Hafner, J. *J. Phys.: Condens. Matter* **1994**, *6*, 8245.
(39) Perdew, J. P.; Wang, Y. *Phys. Rev. B* **1992**, *45*, 13–244.
(40) Monkhorst, H.; Pack, J. D. *Phys. Rev. B* **1976**, *13*, 5188.
(41) Koperski, J.; Atkinson, B.; Krause, L. *Chem. Phys. Lett.* **1994**, *219*, 161.
(42) Liao, M.-S.; Zhang, Q.-E.; Schwarz, W. H. E. *Inorg. Chem.* **1995**, *34*, 5597.
(43) Schwerdtfeger, P.; Boyd, P. D. W.; Brienne, S.; McFeaters, J. S.; Dolg, M.; Liao, M. S.; Schwarz, W. H. E. *Inorg. Chim. Acta* **1993**, *213*, 233.
(44) Kaupp, M.; Vonschnering, H. G. *Inorg. Chem.* **1994**, *33*, 4179.
(45) Stroemberg, D.; Stroemberg, A.; Wahlgren, U. *Water, Air, Soil Pollut.* **1991**, *56*, 681.
(46) Huber, K.-P.; Herzberg, G. *Constants of diatomic molecules; Van Nostrand Reinhold: New York, Toronto* **1979**,
(47) Chase, M. W. *J. Phys. Chem. Ref. Data* **1998**, *Monograph 9*, 1.
(48) Cundari, T. R.; Yoshikawa, A. *J. Comput. Chem.* **1998**, *19*, 902.
(49) Kaupp, M.; Vonschnering, H. G. *Inorg. Chem.* **1994**, *33*, 2555.
(50) Stroemberg, D.; Gropen, O.; Wahlgren, U. *Chem. Phys.* **1989**, *133*, 207.
(51) Liao, M.-S.; Zhang, Q.-E. *Bull. Chem. Soc. Jpn.* **1999**, *72*, 1459.
(52) Givan, A.; Loewenschuss, A. *J. Chem. Phys.* **1976**, *64*, 196.
(53) Whited, R. C.; Flaten, C. J.; Walker, W. C. *Solid State Commun.* **1973**, *13*, 1903.
(54) Medeiros, S. K.; Albuquerque, E. L., Jr.; Caetano, E. W. S.; Farias, G. A.; Freire, V. N.; Cavada, B. S.; Passati, M. L.; Pessati, T. L. P. *Microelectron. J.* **2005**, *36*, 1058.
(55) Sashin, V. A.; Dorsett, H. E.; Bolorizadeh, M. A.; Ford, M. J. *J. Chem. Phys.* **2000**, *113*, 8175.
(56) Elfimoz, I. S.; Yunoki, S.; Sawatzky, G. A. *Phys. Rev. Lett.* **2002**, *89*, 216403.
(57) Medeiros, S. K.; Albuquerque, E. L., Jr.; De Sausa, J. S.; Caetano, E. W. S.; Freire, V. N. *J. Phys. D: Appl. Phys.* **2007**, *40*, 1655.
(58) Baltache, H.; Khenata, R.; Sahnoun, M.; Driz, M.; Abbar, B.; Bouhafs, B. *Physica B* **2004**, *344*, 334.
(59) Anisimov, V. I.; Zaanen, J.; Anderson, O. K. *Phys. Rev. B* **1991**, *44*, 943.
(60) Becke, A. D. *J. Chem. Phys.* **1993**, *98*, 5648.
(61) Rohrbac, A.; Hafner, J.; Kresse, G. *Phys. Rev. B* **2004**, *69*, 075413.
(62) Mosey, N. J.; Carter, E. A. *Phys. Rev. B* **2007**, *76*, 155123.
(63) Yamasaki, A.; Fujiwara, T. *Phys. Rev. B* **2002**, *66*, 245108.
(64) Huang, M.; Fabris, S. *J. Phys. Chem. C* **2008**, *112*, 8643–8648.
(65) Loschen, C.; Carrasco, J.; Neyman, K. M.; Illas, F. *Phys. Rev. B* **2007**, *75*, 035115.
(66) Nolan, M.; Watson, G. W. *Surf. Sci.* **2005**, *586*, 25.
(67) Mehl, M. J.; Hemley, R. J.; Boyer, L. L. *Phys. Rev. B* **1986**, *33*, 8685.

JP801250H